Journal of Integrative Neuroscience

J. Integr. Neurosci. **2026**; 25(11): 55070
https://doi.org/10.31083/JIN55070

Original Research

Immediate Resting-State fNIRS Correlates of Immersion After a Single ARAT-VR Motor Training Session in Healthy Adults: An Exploratory Study

Zhipeng Pan[1,†], Jianxia Lu[2,†], Jingyi Wei[1], Yue Sun[1], Hongrui Liu[1], Boyuan Zhu[3], Cui Yu[2], Guomin Fan[4], Jingyan Cheng[4], Donghe Li[4], Shu Zhu[4], Wei Dou[4], Hewei Wang[4,*], Bin Su[2,*]

[1]School of Rehabilitation, Shandong University of Traditional Chinese Medicine, 250355 Jinan, Shandong, China
[2]School of Rehabilitation, Jiangsu Medical College, 224005 Yancheng, Jiangsu, China
[3]School of Basic Medical Sciences, Changzhi Medical College, 046000 Changzhi, Shanxi, China
[4]Department of Rehabilitation, Huashan Hospital, Fudan University, 200040 Shanghai, China
*Correspondence: wanghew@fudan.edu.cn (Hewei Wang); 13951585359@163.com (Bin Su)
[†]These authors contributed equally.
Academic Editor: Bernat Kocsis
Submitted: 19 June 2026 Revised: 24 July 2026 Accepted: 10 August 2026 Published: 13 November 2026

Abstract

Background: Virtual reality (VR) is increasingly utilized in motor rehabilitation; however, the immediate resting-state hemodynamic and connectivity correlates of highly immersive VR interventions in the human brain remain poorly characterized. In this study, we aimed to investigate short-term cortical reorganization in healthy adults following a single VR-based Action Research Arm Test (ARAT-VR) training session. **Methods:** This exploratory single-arm, pre-post study included 24 healthy adults (19 males, 5 females; mean age: 56.38 ± 5.72 years) without a non-VR or resting control group. Given the exploratory nature, no *a priori* power estimation was conducted. The participants underwent 10 minutes of ARAT-VR upper-limb training. Resting-state functional near-infrared spectroscopy (fNIRS) data were acquired immediately before and after the intervention. Fractional amplitude of low-frequency fluctuation (fALFF) and functional connectivity (FC) were calculated to evaluate the hemodynamic changes associated with the intervention. Brain-behavior correlations and subgroup analyses based on prior VR experience were conducted. **Results:** The ARAT-VR system demonstrated excellent usability and minimal cybersickness. Although global analysis showed no significant mean zfALFF changes, exploratory uncorrected analyses suggested focal hemodynamic modulation trends. Initial analyses showed that the spontaneous activity increments (ΔzfALFF) in the right dorsolateral prefrontal cortex (DLPFC), right primary motor cortex (M1), and left pre-motor/supplementary motor area were positively correlated with subjective immersion scores (uncorrected $p < 0.05$). After controlling for pre-experiment fatigue, cybersickness, and data-quality variation, the immersion-related association remained the most consistent in the right DLPFC, and the motor-region findings were interpreted as exploratory and less stable across analyses. The participants with prior VR exposure showed greater spontaneous activity increments in these regions than novices did (uncorrected $p < 0.05$). Furthermore, exploratory region-of-interest analyses indicated a localized decrease in resting-state FC, highlighted by a decoupling between the left prefrontal and sensorimotor cortices (uncorrected $p = 0.046$). **Conclusions:** In this single-arm study, the observed cortical hemodynamic responses in focal and cortical regions and the localized decreases in resting-state FC are temporally associated with, rather than causally attributable to, the VR intervention. These preliminary, trend-level findings are compatible with a neural-efficiency interpretation, serving as exploratory neuroimaging hypotheses requiring future controlled validation. **Clinical Trial Registration:** No: ChiCTR2500108108. https://www.chictr.org.cn/showproj.html?proj=281157.

Keywords: virtual reality; spectroscopy, near-infrared; brain mapping; neuronal plasticity

1. Introduction

Virtual reality (VR) has become a critical tool in motor training, particularly for upper limb exercises [1,2]. By creating an interactive computer-generated environment, VR allows users to perform movements with high repetition and engagement. Its core advantages include providing goal-driven tasks, high-intensity training doses, adaptive difficulty progression, and real-time kinematic feedback [3,4]. Furthermore, it enhances motivational engagement and increases enjoyment during intensive, task-oriented training [5,6]. These features can significantly motivate users to practice fine motor skills, making VR a widely recognized and effective approach to promote motor learning and neuroplasticity [7,8,9,10].

The Action Research Arm Test (ARAT) is a well-established clinical tool for assessing upper limb function, specifically evaluating fine motor movements such as grasping, gripping, and pinching [11,12,13]. Although it is traditionally employed as an assessment tool, ex-

Copyright: © 2026 The Author(s). Published by IMR Press.
This is an open access article under the CC BY 4.0 license.

Publisher's Note: IMR Press stays neutral with regard to jurisdictional claims in published maps and institutional affiliations.

tracting its core kinematic components to design ARAT-inspired motor training tasks offers a structured and goal-directed framework for VR-based rehabilitation [14]. Functional near-infrared spectroscopy (fNIRS) serves as a practical neuroimaging technique for monitoring upper-limb motor-related hemodynamic changes to investigate the cortical responses associated with these ARAT-inspired tasks [15,16,17,18]. Compared with traditional imaging methods, fNIRS is portable, tolerant of body movements, and does not require a strictly confined environment [19,20], making it particularly suitable for recording cortical activity under natural and interactive conditions.

Neuroimaging studies showed that when healthy subjects perform virtual grasping tasks during VR-based fine motor interactions, their brain activation patterns are highly similar to real physical grasping. In particular, they activate the frontoparietal network (including the pre-motor cortex and inferior parietal lobule) and exhibit normal contralateral activation in the sensorimotor cortex (SMC) with a typical laterality index [21,22]. VR effectively simulates the fundamental neural processes of actual movement, and the virtual environment places unique cognitive and spatial demands on the brain. For example, the selective activation of the angular gyrus and precuneus reflects VR's potential in strengthening body representation and spatial integration [21]. To adapt to these demands, the brain further modulates its network connectivity. Using fNIRS to compare standard and VR grasping, Li et al. [23] found that VR grasping enhanced ipsilateral brain activation and functional connectivity while suppressing contralateral connectivity. This specific modulatory process optimizes the allocation of neural resources, thereby improving overall brain functional efficiency during virtual interactions.

The above findings support the effectiveness of VR training during task execution. However, the long-term benefits of motor training rely on immediate brain activation during the task and how the brain integrates and consolidates neural resources after the training ends [24,25]. Most studies focused on task-state brain activation, paying minimal attention to the "after-effects" that occur once the training is over. Understanding how these training-induced neural changes are maintained and evolve during the resting state is crucial for revealing the dynamic processes of skill consolidation and evaluating resting-state brain network characteristics [26,27]. Furthermore, the neuroplastic effects of VR are not solely determined by the motor task itself but are deeply intertwined with human-computer interaction factors [3]. In particular, virtual immersion and system usability can significantly alter cognitive load and top-down attentional allocation during motor training [28,29]. According to cognitive load theory [30], prior VR experience may critically modulate neural resource allocation. Novices typically consume additional exogenous cognitive resources to adapt to unfamiliar virtual environments, while experienced users can focus directly on motor execution and consolidation [31,32]. How these subjective experiences and prior familiarity quantitatively relate to objective neuroplasticity remains largely unexplored.

Gathering preliminary neurophysiological data from healthy adults is an essential exploratory step before exploring the application of this ARAT-inspired VR training system in clinical populations with motor impairments. Therefore, this study aimed to investigate immediate resting-state hemodynamic responses (i.e., fractional amplitude of low-frequency fluctuation [fALFF] and functional connectivity [FC]) in healthy adults following a single session of ARAT-inspired VR training. Guided by the Neural Efficiency Hypothesis and cognitive load theory, we proposed three *a priori* hypotheses: (1) At the regional level, the VR task will be associated with focal spontaneous activity changes in motor-planning areas (e.g., prefrontal and sensorimotor cortices), and these changes will be positively correlated with subjective immersion (measured by Igroup Presence Questionnaire [IPQ]) and usability (measured by System Usability Scale [SUS]); (2) At the individual level, these regional spontaneous activity increments will be modulated by prior VR experience; and (3) At the network level, FC will exhibit a localized decoupling pattern, potentially reflecting functional pruning during the immediate post-task resting state.

2. Methods

2.1 Participants

Given the pilot and exploratory nature of this neuroimaging investigation, no *a priori* sample size estimation was performed. Twenty-four middle-aged and older healthy adults (nineteen males, five females; age: 56.38 ± 5.72 years; years of education: 9.71 ± 1.68 years) were recruited. The population-level sampling bias inherent in this cohort must be acknowledged. The sex imbalance (79% male) and the narrow education band constitute a specific 'Who You Have Studied' (WYHU) profile. As a consequence, this sampling frame restricts the generalizability of the reported hemodynamic associations to broader adult populations, independent of statistical power constraints. All participants were right-handed, as assessed by the Edinburgh Handedness Inventory. The inclusion and exclusion criteria were rigorously defined (a detailed participant screening and enrollment flowchart is provided in Fig. 1) to minimize confounding physiological factors and ensure data reliability. The detailed demographic characteristics are summarized in Table 1.

Eligible participants were required to meet the following criteria: (1) no history of major neurological, psychiatric, or osteoarticular disorders affecting upper limb motor functions; (2) intact cognitive function, confirmed by a Montreal Cognitive Assessment (MoCA) score ≥26; (3) normal or corrected-to-normal vision and hearing; and (4) no standard VR contraindications (e.g., history of epilepsy, severe motion sickness, or vertigo). Furthermore, all par-

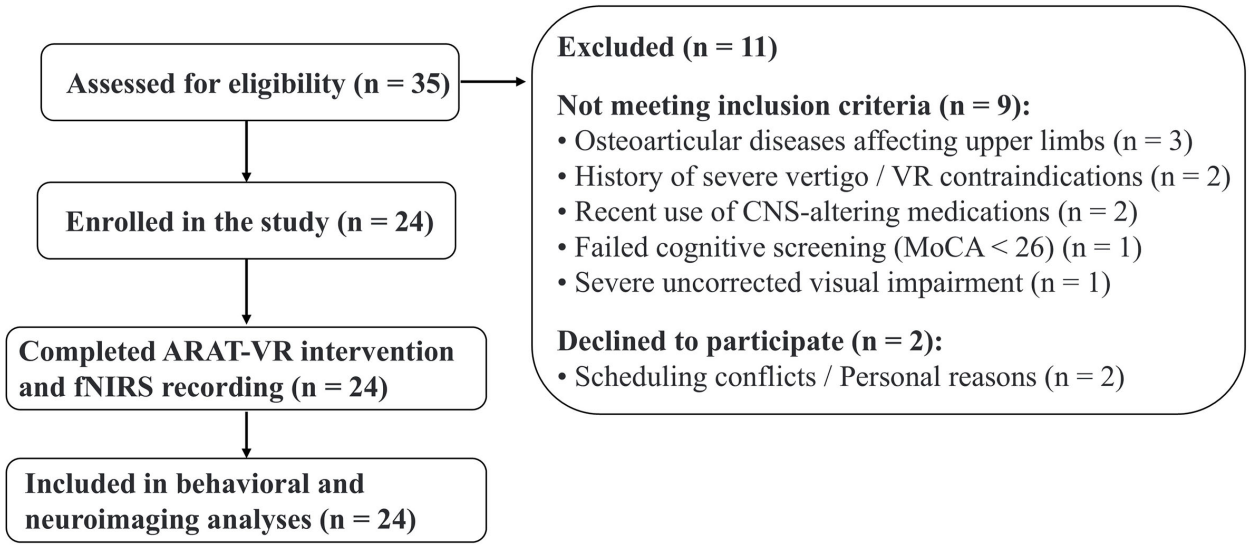


Fig. 1. Participant screening and enrollment flowchart. ARAT-VR, virtual reality-based Action Research Arm Test; fNIRS, functional near-infrared spectroscopy; CNS, central nervous system; MoCA, Montreal Cognitive Assessment.

Table 1. Demographic characteristics, behavioral assessments, and data quality metrics of the participants.

Characteristic	Total (n = 24)	Novice (n = 11)	Experienced (n = 13)	*p*-value [a]
Demographics				
Age (years, mean ± SD)	56.38 ± 5.72	57.73 ± 5.66	55.23 ± 5.69	0.233
Gender (Male/Female)	19/5	8/3	11/2	0.630
Education (years, mean ± SD)	9.71 ± 1.68	9.27 ± 1.68	10.08 ± 1.66	0.073
Behavioral Assessments				
IPQ score	3.48 ± 0.58	3.30 ± 0.49	3.62 ± 0.61	0.191
SUS score	84.46 ± 8.08	83.18 ± 7.50	85.54 ± 8.65	0.281
SSQ score	3.84 ± 1.38	4.09 ± 1.22	3.62 ± 1.39	0.342
Pre-VR fatigue	0.88 ± 0.79	1.00 ± 0.77	0.77 ± 0.83	0.459
Post-VR fatigue	0.83 ± 0.87	0.82 ± 0.87	0.85 ± 0.90	0.621
Fatigue difference (*p*-value) [b]	0.655	0.157	0.083	-
Data Quality Metrics				
Pruned channels per subject	0.79 ± 0.88	0.91 ± 1.04	0.69 ± 0.75	0.290
Motion artifacts per subject	0.58 ± 0.72	0.82 ± 0.87	0.38 ± 0.51	0.304

Note: Continuous variables are presented as mean ± standard deviation (SD). Categorical variables are presented as counts.

[a] *p*-values indicate baseline comparisons between the Novice and Experienced groups (Mann-Whitney U tests for continuous variables; Fisher's exact test for gender).

[b] *p*-values derived from Wilcoxon signed-rank tests comparing pre- and post-VR fatigue within each group (no significant increase in fatigue was observed).

IPQ, Igroup Presence Questionnaire; SUS, System Usability Scale; SSQ, Simulator Sickness Questionnaire.

ticipants were strictly instructed to ensure adequate sleep and abstain from caffeine, alcohol, and any central nervous system-altering medications for at least 24 hours prior to the experiment to control for baseline cerebral hemodynamics. All participants were fully informed and voluntarily signed the informed consent form. Reporting was guided by the STROBE framework where applicable (**Supplementary File 1**).

2.2 Experimental Protocol

The experiment was conducted in a quiet, dimly lit room to minimize environmental distractions. The experimental protocol consisted of three consecutive phases: a pre-training resting state (Pre-VR-Rest), a VR intervention (ARAT-VR training), and an immediate post-training resting state (Post-VR-Rest). During the Pre-VR-Rest phase, the participants were instructed to sit comfortably in a chair,

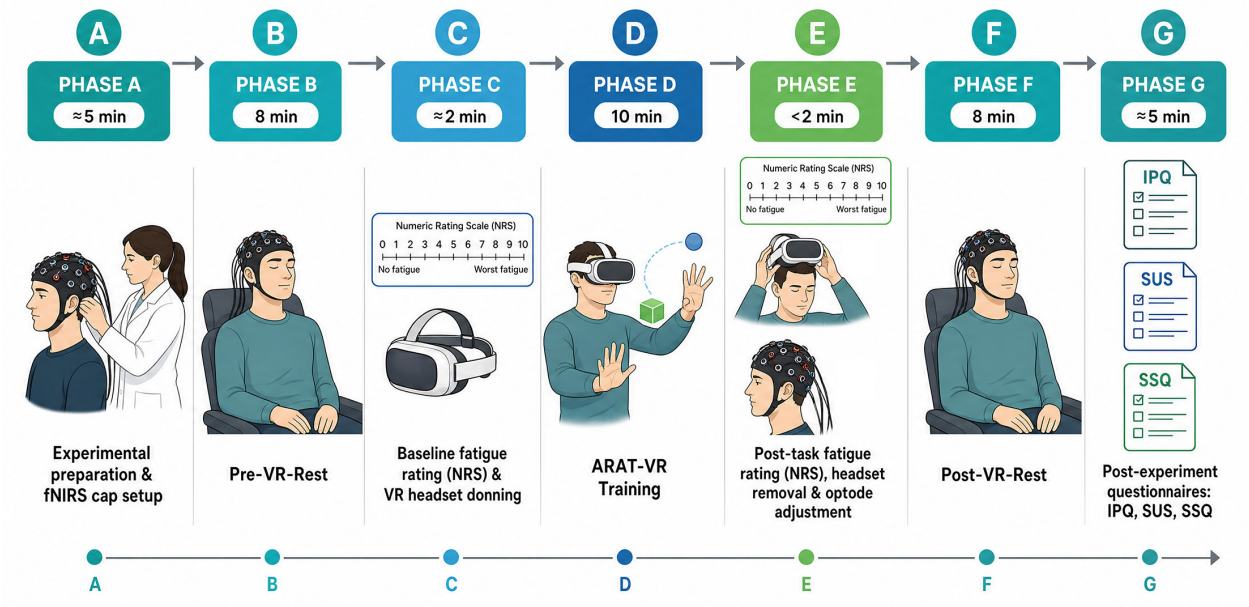


Fig. 2. Schematic of the experimental protocol and data collection timeline. The timeline at the top depicts the chronological sequence with strictly proportional durations for each phase. (A) Experimental preparation and fNIRS cap setup (≈5 min). (B) Initial 8-min resting-state fNIRS acquisition (Pre-VR-Rest, performed with eyes closed and awake). (C) Brief transition phase (≈2 min) wherein the baseline fatigue level was evaluated using an 11-point Numeric Rating Scale (NRS) immediately prior to donning the VR headset. (D) 10-min ARAT-VR intervention, featuring controller-free standardized upper-limb motor tasks. (E) Strict transition interval (<2 min) wherein the immediate post-task fatigue level (NRS) was recorded immediately after removing the VR headset, followed by the re-verification of fNIRS optode coupling. (F) Subsequent 8-min resting-state fNIRS acquisition (Post-VR-Rest, performed with eyes closed and awake). (G) Post-experiment behavioral evaluations (≈5 min), including IPQ, SUS, and SSQ.

keep their eyes closed, relax, and avoid excessive thinking or movement for 8 minutes. Afterward, they performed the standardized ARAT-VR training for 10 minutes. Immediately after the training, the VR headset was removed. The fNIRS cap was strictly adjusted/positioned within a 2-minute time window and carefully re-calibrated using external anatomical landmarks (e.g., the nasion and inion) to maintain precise spatial consistency and minimize the signal variations caused by optode decoupling during the headset removal. Prior to pre–post comparisons within-session z-score standardization was applied to all neuroimaging metrics to mathematically mitigate the potential baseline shifts in absolute light intensity caused by minor cap repositioning. The participants then underwent the 8-minute Post-VR-Rest phase under the same instructions as the baseline (Fig. 2).

2.3 Virtual Reality Intervention

The VR intervention utilized an ARAT-inspired training system developed in Unity 3D (v2021.3, Unity Technologies, San Francisco, CA, USA), with virtual objects spatially modeled upon the standard physical ARAT kit. The system was deployed on a PICO 4 Ultra Enterprise (PICO, Beijing, China) headset operating at a 90 Hz refresh rate. Controller-free interaction was achieved via multi-sensor optical hand tracking (combining 32-megapixel color passthrough and iToF depth sensing), which continuously captured 26 hand key points. Prior to the 10-minute training session, spatial calibration was performed to align the virtual desk with a physical table, establishing visuo-tactile colocation. The training protocol comprised 18 standardized, goal-directed tasks divided into four core subcategories: grasping, gripping, pinching, and gross movements (Fig. 3). Four representative tasks are illustrated in the figure, and the remaining 14 tasks involved systematic variations in object dimensions (e.g., 2.5–10 cm blocks), shapes, and target distances, which were conceptually adapted from the traditional ARAT assessment. A complete and detailed list of all 18 VR tasks, including their physical equivalents and success criteria, is provided in **Supplementary Table 1**. During the 10-minute training block, the participants were instructed to sequentially perform these 18 tasks at a comfortable, self-paced speed. A trial was defined as successful when the virtual object was accurately manipulated, transported to the designated target zone, and stably released without dropping. For robust virtual physics interactions, Proxy Colliders and Continuous Collision Detection algorithms were implemented, accompanied with synchronized audiovisual feedback. No supplemental application-layer kinematic smoothing or artificial target assistance was introduced in our software design.

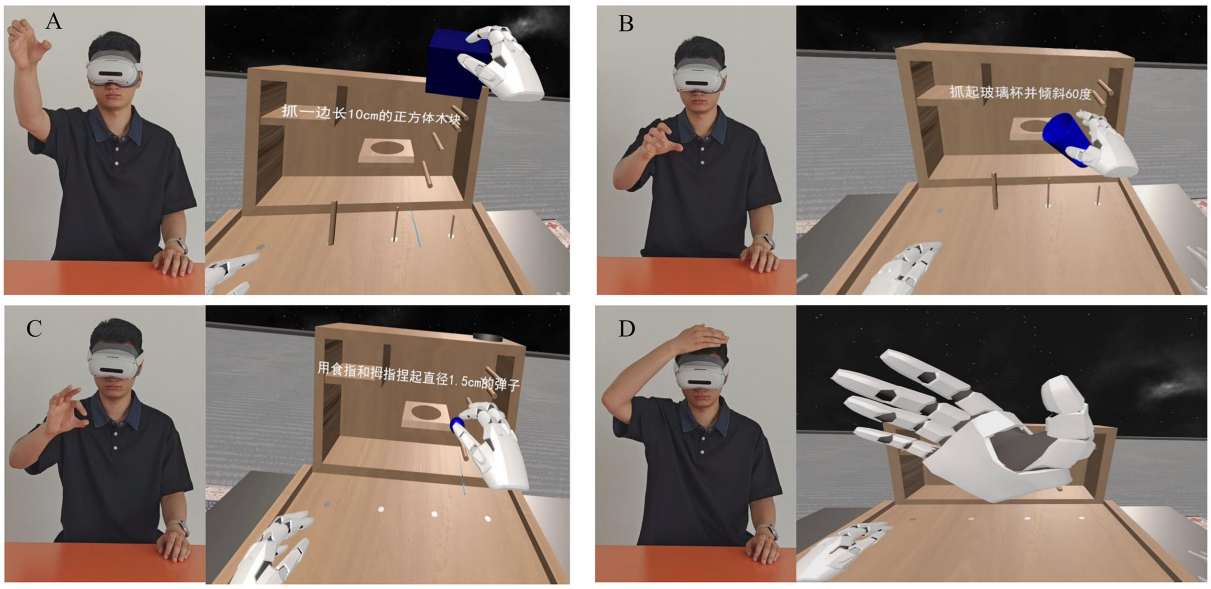


Fig. 3. Representative standardized motor tasks in the ARAT-VR intervention system. The complete VR training protocol comprises 18 standardized upper-limb tasks. Each panel displays the participant's natural kinematics in the real world (left) alongside the corresponding synchronized first-person visual feedback in the virtual environment (right). The system employs controller-free optical hand tracking to ensure high-fidelity interactions. The four illustrated tasks serve as representative examples corresponding to the four core subscales of the Action Research Arm Test (ARAT): (A) Grasping subscale (e.g., reaching and grasping a 10 cm virtual block); (B) Gripping subscale (e.g., gripping a cup and tilting it by 60 degrees); (C) Pinching subscale (e.g., picking up a 1.5 cm marble using the thumb and index finger); and (D) Gross movement subscale (e.g., touching the head).

Subjective interactive experiences were evaluated using three standard questionnaires. Virtual immersion was assessed using the IPQ which comprises 14 items evaluating three subcomponents (Spatial Presence, Involvement, and Experienced Realism) and one general item. The IPQ was reported as a mean score on a 7-point Likert scale to account for the varying number of items across subcomponents. System usability was measured using the 10-item SUS, with raw scores multiplied by the standard factor of 2.5 to yield a composite score ranging from 0 to 100. Cybersickness was monitored via the 16-item Simulator Sickness Questionnaire (SSQ). Given the negligible adverse effects observed in this healthy cohort, the unweighted raw sum score (theoretical range: 0–48) was reported.

Prior VR experience was initially assessed using a 4-level scale (never, 1–2 times, occasionally, frequently). Given the small sample size and sparse responses across the original four-level VR-experience scale, the participants were pragmatically dichotomized into Novice and Experienced groups for exploratory subgroup description. This binary grouping was not intended to represent a validated exposure classification and was interpreted cautiously. Finally, an 11-point Numeric Rating Scale (NRS), with scores ranging from 0 (no fatigue) to 10 (maximum imaginable fatigue), was used to evaluate pre- and post-task subjective fatigue levels.

2.4 fNIRS Data Acquisition

Cortical hemodynamic signals were acquired using a continuous-wave fNIRS system (NirSmart-3000B, Danyang Huichuang Medical Equipment Co., Ltd., Zhenjiang, Jiangsu, China) operating at two near-infrared wavelengths (730 and 850 nm) with a sampling rate of 10 Hz. A customized fNIRS cap was placed on the participant's head, and 18 light sources and 16 detectors were positioned with a standard source-detector separation of 3 cm, yielding 42 effective measurement channels. The optodes were distributed according to the international 10–20 system to specifically cover the prefrontal cortex (PFC) and the sensorimotor cortex (SMC) to ensure strict consistency with our analytical focus.

Regarding spatial localization, given that individual 3D digitization was not available, the anatomical location of each fNIRS channel was estimated using a standard brain template. The spatial coordinates were projected onto the Montreal Neurological Institute (MNI) standard space, and the corresponding Brodmann areas (BAs) were probabilistically estimated using Chris Rorden's MRIcro mapping tool. The anatomical regions and corresponding Brodmann area (BA) labels for the core targeted channels (e.g., DLPFC, premotor/SMA, and M1), together with their exploratory statistical results, are summarized in Table 2.

For all subsequent analyses, oxygenated hemoglobin (HbO) was selected as the primary metric because of its es-

Table 2. Anatomical locations of core channels and statistical results of subgroup comparisons (ΔzfALFF) and Spearman rank correlations with subjective immersion (IPQ).

Channel	Region (BA)	Novice (ΔzfALFF)	Experienced (ΔzfALFF)	Subgroup Diff. (Z, *p*)	Spearman Corr. (ρ, *p*)	Partial Corr. ($r_{partial}$, *p*)
CH31	M1 (BA 4)	–0.19 ± 0.62	0.72 ± 1.01	–2.288, 0.022*	0.444*, 0.030	0.432†, 0.050
CH29	DLPFC (BA 9)	–0.29 ± 1.20	0.78 ± 1.35	–1.999, 0.046*	0.508*, 0.011	0.589**, 0.005
CH12	PMC/SMA (BA 6)	–0.55 ± 1.25	0.49 ± 0.99	–2.173, 0.030*	0.425*, 0.038	0.461*, 0.036
CH9	DLPFC (BA 46)	0.31 ± 0.47	1.36 ± 1.29	–2.057, 0.040*	0.253, 0.233	0.298, 0.190

Note: Data for the Novice and Experienced groups are presented as mean ± standard deviation (SD). Subgroup differences were evaluated via non-parametric Mann-Whitney U tests, with corresponding Z-values reported. Brain-behavior relationships were evaluated via Spearman's rank correlation (ρ). Partial correlations ($r_{partial}$) were conducted while controlling for pre-experiment fatigue, SSQ scores, and number of pruned channels. †indicates $0.05 \leq p < 0.10$ (marginally significant), * indicates $p < 0.05$, ** indicates $p < 0.01$. The core channels showed convergent uncorrected exploratory patterns across subgroup and immersion-related analyses and are highlighted for hypothesis generation. Abbreviations: M1, primary motor cortex; DLPFC, dorsolateral prefrontal cortex; PMC/SMA, pre-motor cortex and supplementary motor area; BA, Brodmann area; ΔzfALFF, standardized spontaneous fractional amplitude of low-frequency fluctuation increments.

tablished sensitivity to task-evoked cortical responses. During data preprocessing, an infinite impulse response (IIR) bandpass filter (0.01–0.08 Hz) was applied to the standard long-separation channel signals. This filtering strategy was utilized to attenuate baseline drifts and systemic physiological artifacts (e.g., cardiac pulsations and respiratory fluctuations).

The 42 channels were clustered *a priori* into four anatomical regions of interest (ROIs) based on prior neuroanatomical knowledge for hypothesis-driven analysis to improve the signal-to-noise ratio (SNR) and rigorously control for multiple comparisons. As illustrated in Fig. 4, the four ROIs were defined as: Left Prefrontal Cortex (LPFC), Right Prefrontal Cortex (RPFC), Left Sensorimotor Cortex (LSMC), and Right Sensorimotor Cortex (RSMC).

2.5 fNIRS Data Preprocessing

Data were preprocessed using the Homer2 (v2.8, Massachusetts General Hospital, Boston, MA, USA) and NIRS-KIT toolboxes (v2.0, Beijing Normal University, Beijing, China) in MATLAB (R2020b, MathWorks, Natick, MA, USA). First raw optical intensity was converted into optical density (OD) using the hmrIntensity2OD function in Homer2. Automated channel pruning was executed using the enPruneChannels function. Channels with an SNR <2.0 or a mean raw optical intensity outside the range of 10^4 – 10^7 were excluded. For each subject, if a channel was pruned in either the pre- or post-VR resting state, then it was excluded from both sessions.

Motion artifacts were identified on a channel-by-channel basis using hmrMotionArtifactByChannel (parameters: tMotion = 0.5 s, tMask = 1.0 s, STDEVthresh = 20.0, AMPthresh = 0.50) and corrected via a spline interpolation algorithm (hmrMotionCorrectSpline, $p = 0.99$). The corrected OD data were converted to HbO and deoxygenated hemoglobin (HbR) concentrations using hmrOD2Conc (modified Beer–Lambert law, differential pathlength factor = [6.0, 6.0]).

HbO signals were selected for all subsequent analyses. The HbO time series was imported into NIRS-KIT and subjected to linear detrending (order = 1). Visual inspection of the continuous time series was additionally performed to exclude remaining severe artifacts. Following detrending, the analytical pipelines diverged for specific metric extraction. For calculating the fALFF, the detrended, non-bandpass-filtered signals were utilized, computing the power ratio of the low-frequency band (0.01–0.08 Hz) to the full detectable frequency range. For calculating FC matrices, an IIR bandpass filter (0.01–0.08 Hz) was explicitly applied to the detrended signals to isolate the resting-state fluctuations.

2.6 Statistical Analysis

Prior to inferential statistics, Shapiro–Wilk test was utilized to evaluate data normality. Raw fALFF and FC values were normalized to zfALFF (Z-score standardization) and zFC (Fisher's r-to-z transformation), respectively. The results indicated that the primary continuous variables did not significantly deviate from a normal distribution ($W = 0.949$–0.969, $p = 0.261$–0.632).

Following a pre-defined statistical protocol, parametric paired *t*-tests were employed for the whole-brain zfALFF mapping. Non-parametric methods, including Spearman's rank correlation, Mann–Whitney U test, and Wilcoxon signed-rank test, were applied for the targeted behavioral correlations, subgroup comparisons, and ROI-wise FC analyses, respectively. Effect sizes (e.g., Cohen's d or rank-biserial correlation) were computed to quantify the magnitude of the statistical comparisons.

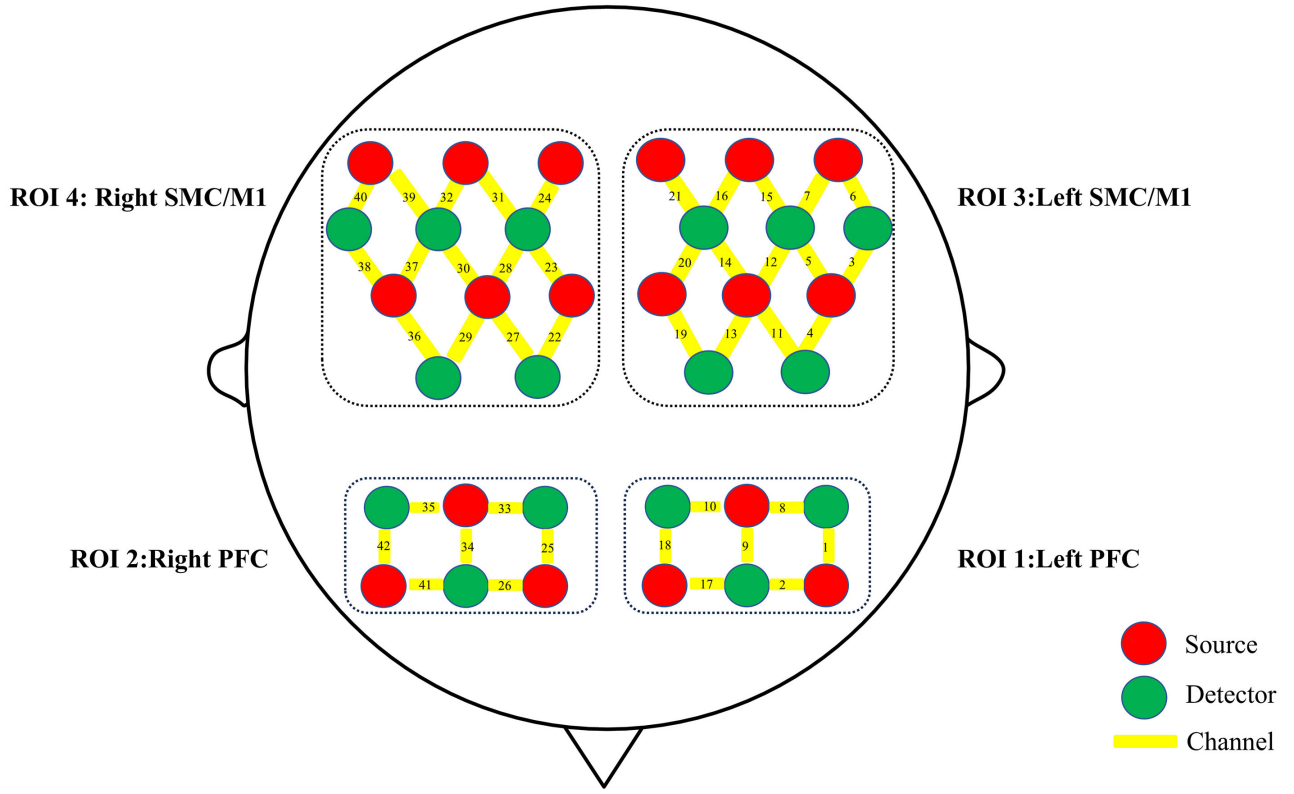


Fig. 4. Spatial arrangement of fNIRS optodes and definition of regions of interest (ROIs). The red and green circles represent the light sources (n = 18) and detectors (n = 16), respectively. The yellow solid lines indicate the 42 effective measurement channels. The layout is displayed from a top-down view (the triangle at the bottom denotes the position of the nasion). The channels were clustered *a priori* into four ROIs, outlined by the dashed boxes, to improve the signal-to-noise and control for multiple comparisons: ROI 1 covers the Left Prefrontal Cortex (left PFC), ROI 2 covers the Right Prefrontal Cortex (right PFC), ROI 3 covers the Left Sensorimotor Cortex/Primary Motor Cortex (left SMC/M1); and ROI 4 covers the Right Sensorimotor Cortex/Primary Motor Cortex (right SMC/M1).

Statistical analyses were conducted using NIRS-KIT and SPSS (v26.0, IBM Corp., Armonk, NY, USA). First, whole-brain paired *t*-test was performed on the zfALFF maps (Post vs. Pre) to evaluate the main effects of the VR intervention. An exploratory framework restricted to predefined anatomical regions of interest, including the prefrontal and sensorimotor cortices, were adopted for subsequent channel-level analyses. Within this predefined anatomical search space, two parallel exploratory analyses were performed. First, Spearman's rank correlation analyses were used to examine associations between channel-wise ΔzfALFF and subjective scale scores (IPQ, SUS, and ΔFatigue). Second, Mann-Whitney U tests were used to compare channel-wise ΔzfALFF between participants with and without prior VR experience. Channels showing convergent patterns across these parallel analyses were interpreted as hypothesis-generating findings rather than confirmatory evidence. Finally, paired *t*-tests were performed on the whole-brain FC matrices, and Wilcoxon signed-rank tests were applied to the ROI-wise zFC matrices.

Partial correlation analyses were conducted between the spontaneous activity increments (ΔzfALFF) of the identified peak channels and the IPQ scores. Pre-experiment fatigue, cybersickness (SSQ scores), and number of pruned channels per subject were entered simultaneously as covariates (degrees of freedom, $df = 19$). Partial correlation coefficients ($r_{partial}$) and their corresponding p-values were computed.

Regarding statistical thresholds, significance for the whole-brain mapping analyses (including the 42-channel zfALFF main effect and 42 × 42 FC matrices) was evaluated using False Discovery Rate (FDR) correction. An exploratory framework restricted to the predefined anatomical search space (the four *a priori* ROIs) were adopted for the subsequent channel-level analyses (i.e., behavioral correlations and subgroup comparisons). These parallel exploratory analyses, along with the specific ROI-wise FC evaluations, were assessed at an uncorrected threshold of $p < 0.05$ (two-tailed).

3. Results

Twenty-four healthy participants completed the experiment. Demographic characteristics, behavioral assessments, and fNIRS data quality metrics for the whole group and the two subgroups (Novice, n = 11; Experienced, n =

13) are summarized in Table 1. For the behavioral assessments, the mean scores for IPQ, SUS, and SSQ were 3.48 ± 0.58, 84.46 ± 8.08, and 3.84 ± 1.38, respectively. Wilcoxon signed-rank tests indicated no significant difference in subjective fatigue levels before and after the experiment (p > 0.05).

Baseline comparisons between the Novice and Experienced groups revealed no significant differences in gender distribution, number of pruned channels, or motion artifacts (all p > 0.05). No significant group differences were identified for age, education years, or behavioral scores (IPQ, SUS, and SSQ) (all p > 0.05).

Initial whole-brain analyses using FDR correction yielded no significant regions or connections. As a consequence, all subsequent neuroimaging results were reported at an uncorrected threshold of p < 0.05 and designated as exploratory trends.

Regarding global cortical activity, paired-samples t-tests across the whole group (N = 24) revealed no significant changes in mean zfALFF values within the four *a priori* ROIs (LPFC, RPFC, LSMC, and RSMC) between the pre- and post-VR resting states (all p > 0.05). Given these null primary results, subsequent analyses were restricted to the predefined anatomical search space (the four ROIs) to explore channel-level hemodynamic modulation trends, which were then visualized through exploratory channel-wise mapping (p < 0.05) (Fig. 5A). Within this predefined anatomical space, two parallel exploratory analyses were conducted.

First, Spearman's rank correlation analyses with 1000-resample bootstrapping were applied to examine the relationship between channel-wise ΔzfALFF and subjective interactive experience within the predefined anatomical search space. This analysis revealed that spontaneous activity increments at specific channels, including the right primary motor cortex (M1; CH31) and right DLPFC (CH29), were positively correlated with the IPQ immersion score (Fig. 5B; uncorrected p = 0.030, 95% bootstrap CI [0.037, 0.739]; and ρ = 0.508, uncorrected p = 0.011, 95% bootstrap CI [0.148, 0.784], respectively). An exploratory positive trend was also observed at the left pre-motor/SMA (CH12) (ρ = 0.425, asymptotic uncorrected p = 0.038), although its 95% bootstrap CI [–0.095, 0.691] included zero, indicating a less robust association. The SUS usability scores exhibited positive correlations with these specific regions (e.g., CH29: ρ = 0.502, uncorrected p = 0.012). A scatter plot illustrating the correlation between IPQ scores and ΔzfALFF at the right DLPFC (CH29) is provided in Fig. 5C, with data points color-coded by subgroup (Novice vs. Experienced).

In the partial correlation analyses (df = 19, controlling for pre-experiment fatigue, SSQ scores, and pruned channels), the correlations between ΔzfALFF and IPQ scores remained significant at the right DLPFC (CH29: $r_{partial}$ = 0.589, p = 0.005) and left pre-motor/SMA (CH12: $r_{partial}$ = 0.461, p = 0.036), while the right M1 (CH31) exhibited a consistent trend ($r_{partial}$ = 0.432, p = 0.050). Bivariate correlation analyses showed that VR-induced cybersickness (SSQ scores) and fatigue had no significant direct correlations with the spontaneous activity increments of these channels (all p > 0.05).

In the parallel exploratory subgroup analysis, nonparametric Mann–Whitney U tests were performed to compare ΔzfALFF between the Novice (n = 11) and Experienced (n = 13) groups. Compared with those in the novice group, the participants with prior VR exposure showed greater exploratory ΔzfALFF trends at the right M1 (CH31; Z = –2.288, p = 0.022), left pre-motor/SMA (CH12; Z = –2.173, p = 0.030), and right DLPFC (CH29; Z = –1.999, p = 0.046) (Fig. 5D). These subgroup differences partially overlapped with the channels showing immersion-related correlations (summarized in Table 2).

Descriptive ΔzfALFF values were stratified by biological sex for the targeted channels to explicitly account for the pronounced sex imbalance in the cohort (19 males vs. 5 females). Males exhibited mean ΔzfALFF changes of 0.65 ± 1.13 at the right DLPFC (CH29), 0.29 ± 0.96 at the right M1 (CH31), and –0.22 ± 1.19 at the left pre-motor/SMA (CH12). Meanwhile, females exhibited mean changes of –1.09 ± 1.43, 0.34 ± 0.88, and 0.92 ± 0.90 in these respective regions.

In addition to regional spontaneous hemodynamic fluctuations, the reorganization of the global FC network, comprising 861 unique edges, was evaluated. Given that no edges survived rigorous multiple comparison corrections (e.g., FDR), an exploratory uncorrected significance matrix (p < 0.05) is illustrated in Fig. 6A to visualize potential network-level trends. The cortical FC network exhibited a highly sparse reorganization pattern, with the majority of the uncorrected significant changes characterized by decreased connectivity strength (negative T-values, blue blocks). This 3D network visualization further highlighted this decreased FC effect (Fig. 6B).

Exploratory ROI-wise analyses suggested specific decoupling trends. In particular, the FC between the LPFC (associated with cognitive control) and LSMC (associated with motor execution) decreased after the VR task (mean ΔzFC = –0.074, Z = –2.000, p = 0.046, effect size r = 0.41). Moreover, the inter-hemispheric connectivity between the bilateral sensorimotor cortices (LSMC-RSMC) also exhibited a reduction (mean ΔzFC = –0.078, Z = –2.143, p = 0.032, effect size r = 0.44). While these localized decoupling patterns aligned with the whole-brain trend of decreased FC, they were evaluated under an uncorrected threshold given their exploratory nature and thus should be interpreted with caution.

4. Discussion

This study investigated the immediate effects of a single VR-based upper limb motor task on resting-state cortical activity in healthy adults using fNIRS. Confirmatory

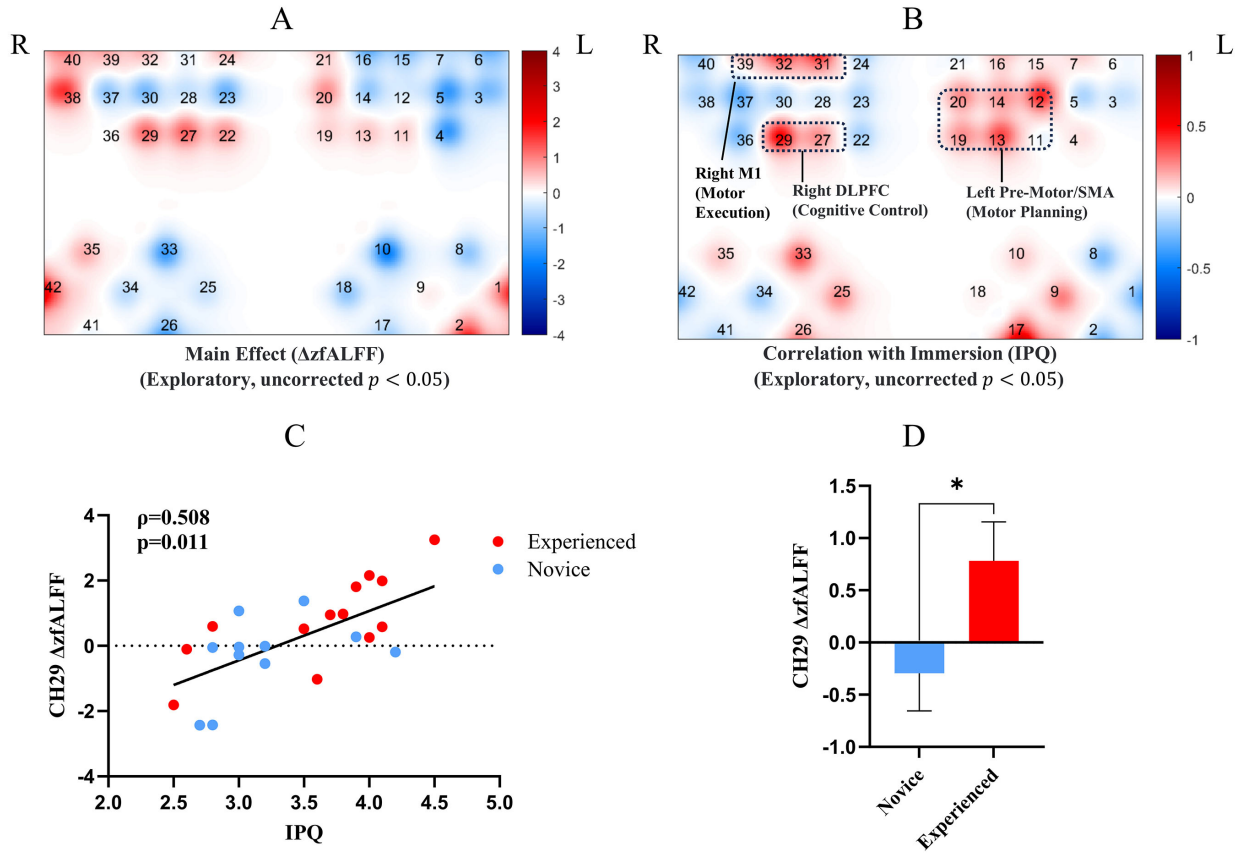


Fig. 5. Regional spontaneous hemodynamic modulation associated with the ARAT-VR intervention and its exploratory brain-behavior mechanisms. (A) Topographical map of ΔzfALFF (Post-VR vs. Pre-VR). The map displays uncorrected channel-wise differences ($p < 0.05$) to illustrate the exploratory trends of regional spontaneous hemodynamic fluctuations. The color bar represents T-values. (B) Channel-wise correlation map between ΔzfALFF and IPQ immersion scores. The map highlights correlations within the *a priori* defined regions of interest (uncorrected $p < 0.05$). (C) Scatter plot demonstrating a significant positive relationship between IPQ scores and the increment of spontaneous hemodynamic fluctuations (ΔzfALFF) at the peak channel located in the right DLPFC (CH29), evaluated via Spearman's rank correlation ($\rho = 0.508$, $p = 0.011$). (D) Subgroup differences associated with prior VR experience. Subgroup analysis reveals that the participants with prior VR exposure showed greater exploratory ΔzfALFF trends at the right DLPFC (CH29) than the novices did (Mann-Whitney U test, $p = 0.046$). Error bars denote the standard error of the mean (SEM). *$p < 0.05$. R, right; L, left.

ROI-level zfALFF showed no significant pre-post change, while subsequent uncorrected channel-wise analyses suggested possible focal associations. On the basis of these exploratory foundations and subsequent targeted evaluations, the findings suggest the following: (1) The VR intervention was associated with localized spontaneous activity trends in specific executive and motor-related regions (e.g., DLPFC, pre-motor/SMA, and primary motor cortex), which were positively correlated with the subjective immersion score. (2) This regional spontaneous hemodynamic fluctuations were associated with prior VR exposure; the participants with prior VR exposure showed greater exploratory ΔzfALFF trends than the novices did. (3) Global FC exhibited a sparse exploratory pattern, characterized by a specific decoupling trend between the prefrontal and sensorimotor cortices.

The positive correlations between ΔzfALFF in the DLPFC, pre-motor/SMA, M1, and IPQ immersion scores suggest a link between the virtual interactive experience and localized cortical responses [33]. DLPFC is recognized as a central hub for executive control and top-down attentional modulation [34], SMA is crucial for complex motor planning [35], and M1 is the primary executor of motor commands [36]. The current results indicate that a high level of immersion may facilitate the recruitment of these specific areas during the subsequent resting state, potentially reflecting post-task resting-state hemodynamic modulation [24,25]. Although such spontaneous regional activity changes are theoretically associated with early motor memory consolidation, the absence of behavioral retention or transfer tests in the current design means that this relationship remains a hypothesis to be rigorously tested in

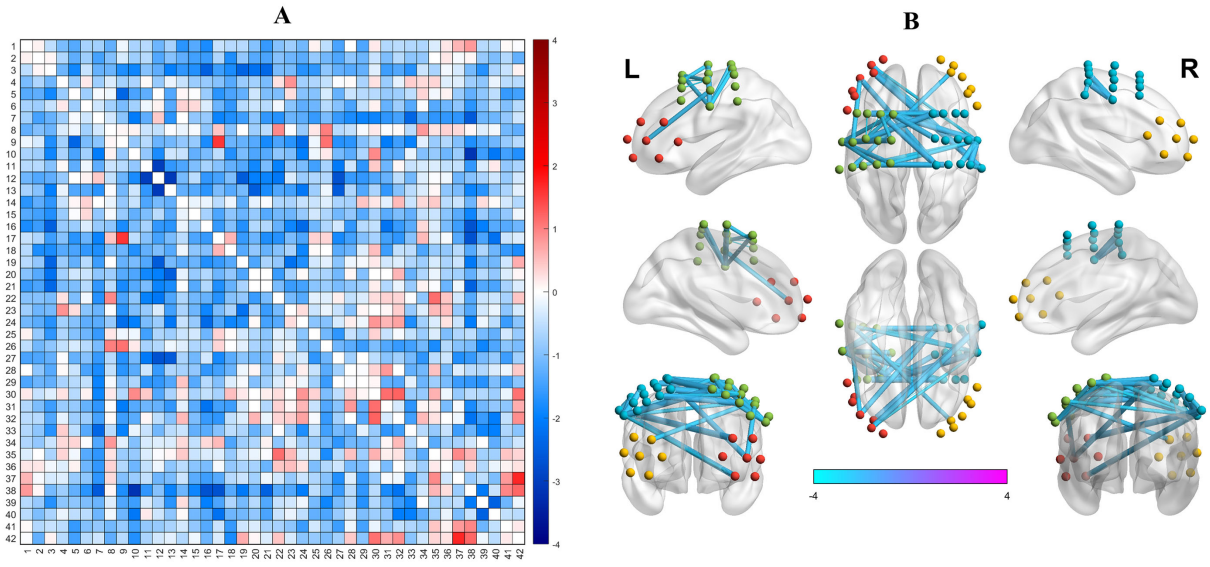


Fig. 6. Exploratory decreases in resting-state functional connectivity following the ARAT-VR intervention. (A) 42 × 42 uncorrected T-statistic matrix of functional connectivity (FC) changes (Post-VR vs. Pre-VR). The color bar represents T-values (ranging from –4 to 4). The predominant presence of blue blocks (T <0) indicates a consistent trend of decreased inter-channel connectivity. (B) Spherical nodes representing the 42 fNIRS channels mapped onto the MNI standard brain template. Nodes are color-coded to delineate the four *a priori* ROIs: Left Prefrontal Cortex (LPFC, red), Right Prefrontal Cortex (RPFC, orange), Left Sensorimotor Cortex (LSMC, green), and Right Sensorimotor Cortex (RSMC, blue). Edge selection rules: The edges (connecting lines) illustrate decreases in FC between channel pairs. Significance was evaluated at an exploratory uncorrected threshold of $p < 0.05$ (corresponding to T <–2.06 for $df = 23$). As no edges survived FDR correction, this visualization represents an exploratory network trend. The cool color gradient and the thickness of the edges encode the absolute T-values (ranging from |–2.06| to |–3.18|), visually highlighting the localized decoupling at post-intervention.

future longitudinal studies. Furthermore, the lack of significant correlations between ΔzfALFF and fatigue or SSQ scores helps exclude the potential confounding effects of physiological exhaustion or cybersickness [37], suggesting that the observed changes are primarily related to the VR task itself [3]. Partial correlation analysis was conducted while controlling for pre-experiment fatigue, cybersickness (SSQ scores), and data quality variations (number of pruned channels per subject). The positive correlations with IPQ immersion remained statistically significant at the right DLPFC and left pre-motor/SMA, the right M1 exhibited a similar positive trend. This sensitivity analysis suggests that focal spontaneous hemodynamic fluctuations are associated with the immersive VR experience, independent of the measured physiological and data quality covariates.

Subgroup analyses revealed that prior VR exposure was associated with different regional fALFF changes [31]. While the current experimental design lacked continuous cognitive load monitoring or objective retention tests to definitively establish the underlying behavioral mechanisms, the observed neural variance provides a compelling theoretical basis for discussion. Although the participants with prior VR exposure showed greater exploratory ΔzfALFF trends in spontaneous hemodynamic fluctuations within these *a priori* target regions compared with the novices, explanations based on varying levels of cognitive load [28,29] or neural resource allocation remain speculative. The hypothesis is that for novices, adapting to an unfamiliar virtual environment might introduce additional cognitive demands [38,39,40], potentially diverting attention toward spatial orientation and environmental adaptation rather than motor execution [41]. By contrast, the participants with prior VR exposure might automatically navigate the VR environment [42], theoretically influencing subsequent post-task spontaneous neural patterns [32,43,44]. This experience-dependent variance aligned with previous functional neuroimaging studies on motor learning, which indicated that the initial stages of learning (e.g., novices) typically require widespread frontoparietal recruitment to cope with high cognitive demands, whereas advanced stages (e.g., participants with prior VR exposure) shift towards localized, specialized motor network activation [31,42]. While these findings aligned with the principles of experience-dependent resource allocation, direct behavioral corroboration is necessary to transition these concepts from exploratory hypotheses to confirmed mechanisms in future studies. Nevertheless, the spatial overlap between these parallel analyses is noteworthy. It suggests a convergent but exploratory pattern linking subjective immersion, prior VR exposure, and localized post-task hemodynamic modulation.

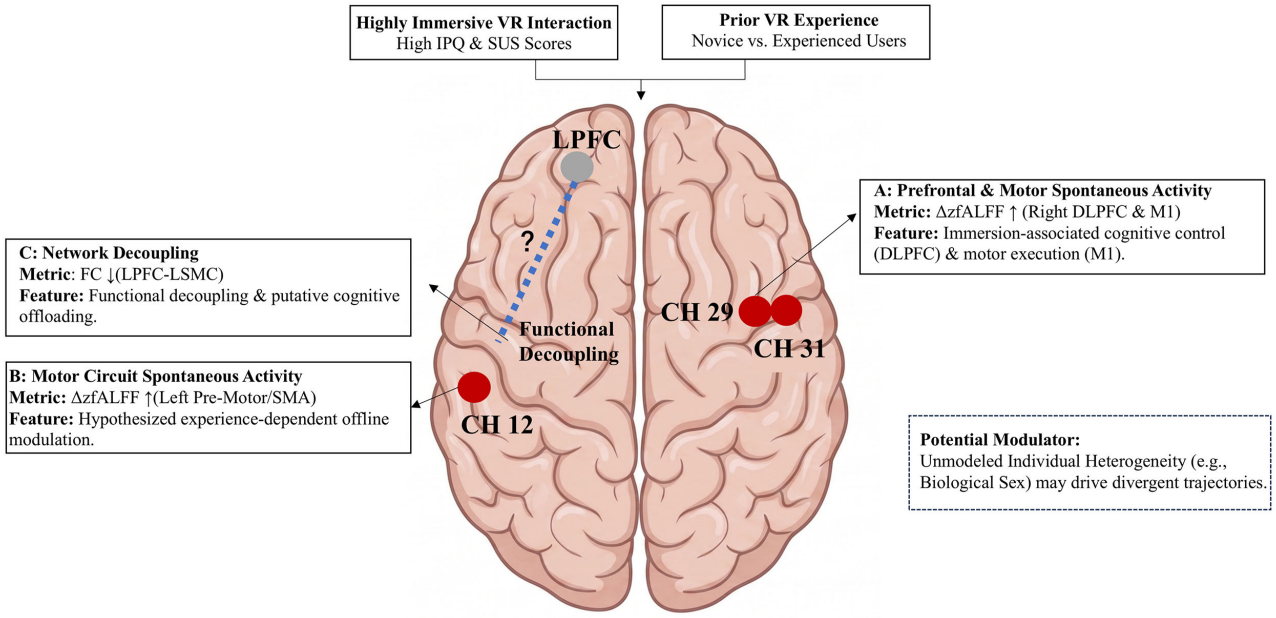


Fig. 7. Proposed exploratory framework outlining the putative associations following the immersive ARAT-VR intervention. This conceptual model is hypothesis-generating. The dashed lines indicate putative associations that require future empirical validation. (A) Immersion-associated prefrontal and motor spontaneous activity: The ΔzfALFF in the right DLPFC (CH29) and right primary motor cortex (M1; CH31) (red nodes) exhibited an exploratory trend of spontaneous activity increments (uncorrected $p < 0.05$), both exhibiting positive correlations with subjective immersion (IPQ scores). (B) Experience-dependent motor spontaneous activity: The left pre-motor/SMA (CH12, red node) exhibited focal spontaneous activity increments that were associated with prior VR experience. (C) Intra-hemispheric network decoupling: The reduction in functional connectivity (blue dashed line) between the LPFC (grey node) and the LSMC suggests an exploratory trend of decreased network communication. Note: This conceptual framework represents a group-level aggregate pattern. As indicated by the dashed modulator box, this uniform pathway may obscure divergent, individual-level neurobiological trajectories driven by unmodeled heterogeneity (e.g., biological sex).

In addition to prior VR experience, the potential influence of unmodeled individual neurobiological heterogeneity warrants consideration. The descriptive results indicated that the spontaneous activity increments (ΔzfALFF) exhibited divergent response patterns between males and females across the targeted regions (e.g., opposing polarities in the DLPFC and SMA). Recent variance-partitioning studies suggested that biological sex may account for substantial variance in regional prefrontal-motor activity, contributing to divergent, individual-level reorganization trajectories [45]. As a consequence, the immersion-associated correlations observed in the overall sample may be structurally confounded by this sex-related heterogeneity. This variance highlights the relevance of a 'dual diversity' framework in interpreting neuroergonomic data, suggesting that aggregate group-level patterns may obscure underlying individual physiological differences.

In addition to regional spontaneous hemodynamic fluctuations, the whole-brain functional connectivity matrix revealed a general decrease in inter-channel communication, indicating a sparse reorganization of the functional brain network architecture [46]. Supported by this whole-brain trend, our exploratory ROI-wise non-parametric analysis revealed significant decoupling between the LPFC (associated with cognitive control) and LSMC (associated with motor execution) ($p = 0.046$) between the bilateral sensorimotor cortices (LSMC-RSMC, $p = 0.032$). One possible explanatory framework for this dual-decoupling pattern is the "Neural Efficiency Hypothesis" [47,48,49]. Within this context, as participants adapt to the VR motor interactions, the reliance on prefrontal cognitive control may decrease (cognitive offloading), and inter-hemispheric crosstalk may be minimized. This process could theoretically reduce background noise and provide a highly focused, lateralized physiological state for motor skill consolidation [27,50,51]. Furthermore, the observed decoupling pattern was supported by prior studies on resting-state functional magnetic resonance imaging (fMRI)/fNIRS motor learning. Motor practice induces significant resting-state network decoupling between cognitive control hubs (e.g., prefrontal cor-

tex) and primary sensorimotor areas. This topological reorganization reflects a transition from effortful cognitive monitoring to motor automaticity [25,50]. However, alternative non-neural explanations for this decreased FC must be carefully considered. The observed general reduction might also arise from inadequate regression of global physiological noise [52,53], post-motor autonomic nervous system fluctuations [54], decreased vigilance during the second resting state [55], alterations in superficial scalp blood flow [56], or minor differences in optode coupling after removing the VR headset [57]. These specific decoupling patterns were evaluated under an uncorrected threshold. Given the exploratory nature of this ROI-wise analysis and the aforementioned systemic confounders, these findings should be interpreted with strict caution. Rather than establishing a definitive neural-efficiency mechanism, they provide preliminary, hypothesis-generating data that warrant rigorous validation in future studies incorporating short-separation channels and larger sample sizes [53,56].

By integrating the findings, we present a hypothesis-generating conceptual framework to illustrate the putative immediate after-effects of VR motor training on resting-state brain activity (Fig. 7). This proposed exploratory model suggests that immersive interactive experiences may be associated with targeted regional spontaneous hemodynamic fluctuations, a process that is hypothetically modulated by prior VR experience during the post-task resting state [24]. At the same time, the observed intra-hemispheric decoupling might reflect an effect of decreased FC, which is theorized to help minimize background noise as participants adapt to the motor task. Overall, this concurrent pattern of focal spontaneous hemodynamic fluctuations and functional decoupling aligns with the principles of the "Neural Efficiency Hypothesis" [48,49], pointing toward a proposed physiological state that may support optimal motor skill acquisition; however, this finding remains to be definitively verified.

While these findings in healthy adults provide valuable insights, they cannot be directly extrapolated to clinical populations such as stroke survivors. Patients who experience stroke present with highly complex and heterogeneous clinical profiles, including structural brain lesions, neuroplastic compensatory mechanisms, altered neurovascular coupling, and varying degrees of cognitive impairment and fatigue, all of which may be further confounded by pharmacological treatments [58,59,60]. Therefore, the current results should be interpreted strictly as hypotheses for future patient studies. On the basis of our observations, we hypothesize that optimizing the immersive quality of VR systems may facilitate the engagement of target motor networks in patients. We also hypothesize that a pre-training familiarization period might be necessary for patients with no prior VR experience to mitigate excessive cognitive load and optimize neuroplastic effects [61]. Future clinical validation studies should employ longitudinal randomized controlled designs to rigorously test these hypotheses. Clinical behavioral assessments must be integrated with multimodal neuroimaging (e.g., incorporating structural magnetic resonance imaging (MRI) to account for lesion load and fNIRS/electroencephalography [EEG] for cortical activity) to monitor stroke survivors across multiple VR sessions, explicitly controlling for baseline cognitive reserve, fatigue levels, and prior technology exposure.

5. Limitations

Several limitations emphasize the exploratory nature of this study. First, the single-arm, pre-post design lacked a non-VR or sham control. As a consequence, the observed pre-post hemodynamic changes cannot be unequivocally attributed to the VR session; they may equally reflect time-related drift, repeated-measurement effects, habituation, or expectancy. This restricts our findings to temporal associations rather than causal inferences.

Second, the relatively small sample (N = 24) lacked sufficient power for reliable multi-covariate adjustments, and all targeted channel- and network-level analyses were evaluated at uncorrected thresholds ($p < 0.05$). The severe gender imbalance (19 males vs. 5 females) and narrow education band represent a distinct WYHU sampling bias, restricting generalizability and acting as a significant source of unmodeled individual neurobiological heterogeneity. Future studies must employ sex-stratified recruitment and incorporate *a priori* biological sex to uncouple these complex effects.

Third, the fNIRS interpretations are constrained by the exclusive reliance on HbO signals, lack of short-separation channels for systemic noise regression, and potential optode coupling variations introduced during VR headset removal. Fourth, behavioral evaluations relied entirely on subjective reports. Pragmatically dichotomizing the sparse prior VR experience data into a binary split, combined with uncorrected channel-wise comparisons, carries a high risk of type I error. Finally, the absence of continuous cognitive load monitoring, objective kinematic validation, and longitudinal retention tests means that our mechanistic hypotheses remain speculative. Extrapolating these healthy-baseline findings to stroke survivors requires extreme caution because of complex neurovascular pathologies, necessitating future rigorous randomized controlled trials.

6. Conclusion

Within the context of this exploratory single-arm study, the 10-minute ARAT-inspired VR session was temporally associated with, rather than causally attributable to, preliminary trends in resting-state cortical activity and FC. While ROI-averaged zfALFF was not significantly altered, uncorrected channel-level analyses pointed to putative associations between subjective immersion and localized spontaneous hemodynamic fluctuations in motor-planning areas and alongside possible global network func-

tional decoupling. These preliminary results offer an objective, albeit exploratory, neuroimaging perspective on the immediate effects of VR-based motor tasks.

Availability of Data and Materials

The datasets generated and analyzed during the current study are available from the corresponding authors on reasonable request.

Author Contributions

ZP conducted the formal analysis and wrote the original draft. JL contributed to the methodology and investigation. JW performed the investigation, and YS assisted with the formal analysis. HL was responsible for data curation, while BZ developed the software. CY contributed to data validation. GF, JC, DL, SZ, and WD contributed to data curation and assisted with manuscript writing and revision. HW contributed to conceptualization, supervised the research, and managed project administration. BS contributed to conceptualization, acquired funding, supervised the research, and reviewed and edited the manuscript. All authors contributed to editorial changes in the manuscript. All authors read and approved the final manuscript. All authors have participated sufficiently in the work and agreed to be accountable for all aspects of the work.

Ethics Approval and Consent to Participate

The overarching ARAT-VR research project was registered with the Chinese Clinical Trial Registry (ChiCTR2500108108; Registration Date: August 25, 2025). The present exploratory study in healthy adults was conducted as a preliminary component of this broader project and was not separately registered. The study was conducted in accordance with the Declaration of Helsinki.

Acknowledgment

We sincerely thank all investigators, assessors and participants for their joint contributions to this trial.

Funding

This project is being supported by Jiangsu Medical College Research Start-up Funding Project (20256106), Jiangsu Medical College's Leading Talent Cultivation Support Program (000520240111), Rehabilitation Education Reform and Innovation Team Development Project (000520241028), Key Medical Research Project of Jiangsu Commission of Health (K2025027), Yancheng Brain Health and Intelligent Rehabilitation Engineering and Technology Research Centre (YC2025609), China National Nature Science Young Foundation (82102665), Shanghai Sailing Program (21YF1404600).

Conflicts of Interest

The authors declare no conflicts of interest.

Supplementary Material

Supplementary material associated with this article can be found, in the online version, at https://doi.org/10.31083/JIN55070.

References

[1] Javvaji CK, Reddy H, Vagha JD, Taksande A, Kommareddy A, Reddy NS. Immersive Innovations: Exploring the Diverse Applications of Virtual Reality (VR) in Healthcare. Cureus. 2024; 16: e56137. https://doi.org/10.7759/cureus.56137

[2] Wang Y, Zhu M, Chen X, Liu R, Ge J, Song Y, et al. The application of metaverse in healthcare. Frontiers in Public Health. 2024; 12: 1420367. https://doi.org/10.3389/fpubh.2024.1420367

[3] Levin MF, Weiss PL, Keshner EA. Emergence of virtual reality as a tool for upper limb rehabilitation: incorporation of motor control and motor learning principles. Physical Therapy. 2015; 95: 415–425. https://doi.org/10.2522/ptj.20130579

[4] Maier M, Rubio Ballester B, Duff A, Duarte Oller E, Verschure PFMJ. Effect of Specific Over Nonspecific VR-Based Rehabilitation on Poststroke Motor Recovery: A Systematic Meta-analysis. Neurorehabilitation and Neural Repair. 2019; 33: 112–129. https://doi.org/10.1177/1545968318820169

[5] Lansberg MG, Legault C, MacLellan A, Parikh A, Muccini J, Mlynash M, et al. Home-based virtual reality therapy for hand recovery after stroke. PM & R: the Journal of Injury, Function, and Rehabilitation. 2022; 14: 320–328. https://doi.org/10.1002/pmrj.12598

[6] Perez-Marcos D, Chevalley O, Schmidlin T, Garipelli G, Serino A, Vuadens P, et al. Increasing upper limb training intensity in chronic stroke using embodied virtual reality: a pilot study. Journal of Neuroengineering and Rehabilitation. 2017; 14: 119. https://doi.org/10.1186/s12984-017-0328-9

[7] Ballester BR, Nirme J, Camacho I, Duarte E, Rodríguez S, Cuxart A, et al. Domiciliary VR-Based Therapy for Functional Recovery and Cortical Reorganization: Randomized Controlled Trial in Participants at the Chronic Stage Post Stroke. JMIR Serious Games. 2017; 5: e15. https://doi.org/10.2196/games.6773

[8] Xu G, Huo C, Yin J, Li W, Xie H, Li X, et al. Effective brain network analysis in unilateral and bilateral upper limb exercise training in subjects with stroke. Medical Physics. 2022; 49: 3333–3346. https://doi.org/10.1002/mp.15570

[9] Xu S, Xu Y, Wen R, Wang J, Qiu Y, Chan CC. Virtual Reality Enhanced Exercise Training in Upper Limb Function of Patients With Stroke: Meta-Analytic Study. Journal of Medical Internet Research. 2025; 27: e66802. https://doi.org/10.2196/66802

[10] Zhang B, Li D, Liu Y, Wang J, Xiao Q. Virtual reality for limb motor function, balance, gait, cognition and daily function of stroke patients: A systematic review and meta-analysis. Journal of Advanced Nursing. 2021; 77: 3255–3273. https://doi.org/10.1111/jan.14800

[11] Lyle RC. A performance test for assessment of upper limb function in physical rehabilitation treatment and research. International Journal of Rehabilitation Research. Internationale Zeitschrift Fur Rehabilitationsforschung. Revue Internationale De Recherches De Readaptation. 1981; 4: 483–492. https://doi.org/10.1097/00004356-198112000-00001

[12] Platz T, Pinkowski C, van Wijck F, Kim IH, di Bella P, Johnson G. Reliability and validity of arm function assessment with standardized guidelines for the Fugl-Meyer Test, Action Research Arm Test and Box and Block Test: a multicentre study. Clinical Rehabilitation. 2005; 19: 404–411. https://doi.org/10.1191/0269215505cr832oa

[13] Pohl J, Held JPO, Verheyden G, Alt Murphy M, Engelter S, Flöel A, et al. Consensus-Based Core Set of Outcome Measures

for Clinical Motor Rehabilitation After Stroke-A Delphi Study. Frontiers in Neurology. 2020; 11: 875. https://doi.org/10.3389/fneur.2020.00875

[14] Burton Q, Lejeune T, Dehem S, Lebrun N, Ajana K, Edwards MG, et al. Performing a shortened version of the Action Research Arm Test in immersive virtual reality to assess post-stroke upper limb activity. Journal of Neuroengineering and Rehabilitation. 2022; 19: 133. https://doi.org/10.1186/s12984-022-01114-3

[15] Chen WL, Wagner J, Heugel N, Sugar J, Lee YW, Conant L, et al. Functional Near-Infrared Spectroscopy and Its Clinical Application in the Field of Neuroscience: Advances and Future Directions. Frontiers in Neuroscience. 2020; 14: 724. https://doi.org/10.3389/fnins.2020.00724

[16] Cui Y, Cong F, Huang FB, Zeng M, Wang J. Effects of Electrical Stimulation on Activation of Mirror Neuron Network in Healthy Adults during Motor Execution and Imitation: An fNIRS Study. Journal of Integrative Neuroscience. 2025; 24: 25731. https://doi.org/10.31083/JIN25731

[17] Ferrari M, Quaresima V. A brief review on the history of human functional near-infrared spectroscopy (fNIRS) development and fields of application. NeuroImage. 2012; 63: 921–935. https://doi.org/10.1016/j.neuroimage.2012.03.049

[18] Zhou Y, Xie H, Li X, Huang W, Wu X, Zhang X, et al. Predicting upper limb motor recovery in subacute stroke patients via fNIRS-measured cerebral functional responses induced by robotic training. Journal of Neuroengineering and Rehabilitation. 2024; 21: 226. https://doi.org/10.1186/s12984-024-01523-6

[19] Pinti P, Tachtsidis I, Hamilton A, Hirsch J, Aichelburg C, Gilbert S, et al. The present and future use of functional near-infrared spectroscopy (fNIRS) for cognitive neuroscience. Annals of the New York Academy of Sciences. 2020; 1464: 5–29. https://doi.org/10.1111/nyas.13948

[20] Zhao YN, Han PP, Zhang XY, Bi X. Applications of Functional Near-Infrared Spectroscopy (fNIRS) Neuroimaging During Rehabilitation Following Stroke: A Review. Medical Science Monitor: International Medical Journal of Experimental and Clinical Research. 2024; 30: e943785. https://doi.org/10.12659/MSM.943785

[21] Adamovich SV, August K, Merians A, Tunik E. A virtual reality-based system integrated with fmri to study neural mechanisms of action observation-execution: a proof of concept study. Restorative Neurology and Neuroscience. 2009; 27: 209–223. https://doi.org/10.3233/RNN-2009-0471

[22] Jang SH, You SH, Hallett M, Cho YW, Park CM, Cho SH, et al. Cortical reorganization and associated functional motor recovery after virtual reality in patients with chronic stroke: an experimenter-blind preliminary study. Archives of Physical Medicine and Rehabilitation. 2005; 86: 2218–2223. https://doi.org/10.1016/j.apmr.2005.04.015

[23] Li X, Yin J, Li H, Xu G, Huo C, Xie H, et al. Effects of Ordered Grasping Movement on Brain Function in the Performance Virtual Reality Task: A Near-Infrared Spectroscopy Study. Frontiers in Human Neuroscience. 2022; 16: 798416. https://doi.org/10.3389/fnhum.2022.798416

[24] Albert NB, Robertson EM, Miall RC. The resting human brain and motor learning. Current Biology: CB. 2009; 19: 1023–1027. https://doi.org/10.1016/j.cub.2009.04.028

[25] Vahdat S, Darainy M, Milner TE, Ostry DJ. Functionally specific changes in resting-state sensorimotor networks after motor learning. The Journal of Neuroscience: the Official Journal of the Society for Neuroscience. 2011; 31: 16907–16915. https://doi.org/10.1523/JNEUROSCI.2737-11.2011

[26] Bernardi NF, Van Vugt FT, Valle-Mena RR, Vahdat S, Ostry DJ. Error-related Persistence of Motor Activity in Resting-state Networks. Journal of Cognitive Neuroscience. 2018; 30: 1883–1901. https://doi.org/10.1162/jocn_a_01323

[27] Taubert M, Lohmann G, Margulies DS, Villringer A, Ragert P. Long-term effects of motor training on resting-state networks and underlying brain structure. NeuroImage. 2011; 57: 1492–1498. https://doi.org/10.1016/j.neuroimage.2011.05.078

[28] Fishburn FA, Norr ME, Medvedev AV, Vaidya CJ. Sensitivity of fNIRS to cognitive state and load. Frontiers in Human Neuroscience. 2014; 8: 76. https://doi.org/10.3389/fnhum.2014.00076

[29] Makransky G, Terkildsen TS, Mayer RE. Adding immersive virtual reality to a science lab simulation causes more presence but less learning. Learning and Instruction. 2019; 60: 225–236. https://doi.org/10.1016/j.learninstruc.2017.12.007

[30] Sweller J. Cognitive load theory. In Ross BH (ed.) Psychology of learning and motivation (pp. 37–76). Elsevier: San Diego, CA, USA. 2011.

[31] Kelly AMC, Garavan H. Human functional neuroimaging of brain changes associated with practice. Cerebral Cortex (New York, N.Y.: 1991). 2005; 15: 1089–1102. https://doi.org/10.1093/cercor/bhi005

[32] Wu T, Kansaku K, Hallett M. How self-initiated memorized movements become automatic: a functional MRI study. Journal of Neurophysiology. 2004; 91: 1690–1698. https://doi.org/10.1152/jn.01052.2003

[33] Kober SE, Kurzmann J, Neuper C. Cortical correlate of spatial presence in 2D and 3D interactive virtual reality: an EEG study. International Journal of Psychophysiology: Official Journal of the International Organization of Psychophysiology. 2012; 83: 365–374. https://doi.org/10.1016/j.ijpsycho.2011.12.003

[34] MacDonald AW, 3rd, Cohen JD, Stenger VA, Carter CS. Dissociating the role of the dorsolateral prefrontal and anterior cingulate cortex in cognitive control. Science (New York, N.Y.). 2000; 288: 1835–1838. https://doi.org/10.1126/science.288.5472.1835

[35] Hardwick RM, Rottschy C, Miall RC, Eickhoff SB. A quantitative meta-analysis and review of motor learning in the human brain. NeuroImage. 2013; 67: 283–297. https://doi.org/10.1016/j.neuroimage.2012.11.020

[36] Sanes JN, Donoghue JP. Plasticity and primary motor cortex. Annual Review of Neuroscience. 2000; 23: 393–415. https://doi.org/10.1146/annurev.neuro.23.1.393

[37] Kennedy RS, Lane NE, Berbaum KS, Lilienthal MG. Simulator sickness questionnaire: An enhanced method for quantifying simulator sickness. The International Journal of Aviation Psychology. 1993; 3: 203–220. https://doi.org/10.1207/s15327108ijap0303_3

[38] Bohil CJ, Alicea B, Biocca FA. Virtual reality in neuroscience research and therapy. Nature Reviews. Neuroscience. 2011; 12: 752–762. https://doi.org/10.1038/nrn3122

[39] Gramann K, Onton J, Riccobon D, Mueller HJ, Bardins S, Makeig S. Human brain dynamics accompanying use of egocentric and allocentric reference frames during navigation. Journal of Cognitive Neuroscience. 2010; 22: 2836–2849. https://doi.org/10.1162/jocn.2009.21369

[40] Parong J, Mayer RE. Learning science in immersive virtual reality. Journal of Educational Psychology. 2018; 110: 785. https://doi.org/10.1037/edu0000241

[41] Mandrick K, Derosiere G, Dray G, Coulon D, Micallef JP, Perrey S. Prefrontal cortex activity during motor tasks with additional mental load requiring attentional demand: a near-infrared spectroscopy study. Neuroscience Research. 2013; 76: 156–162. https://doi.org/10.1016/j.neures.2013.04.006

[42] Poldrack RA, Sabb FW, Foerde K, Tom SM, Asarnow RF, Bookheimer SY, et al. The neural correlates of motor skill automaticity. The Journal of Neuroscience: the Official Journal of the Society for Neuroscience. 2005; 25: 5356–5364. https:

//doi.org/10.1523/JNEUROSCI.3880-04.2005
[43] Chein JM, Schneider W. Neuroimaging studies of practice-related change: fMRI and meta-analytic evidence of a domain-general control network for learning. Brain Research. Cognitive Brain Research. 2005; 25: 607–623. https://doi.org/10.1016/j.cogbrainres.2005.08.013
[44] Puttemans V, Wenderoth N, Swinnen SP. Changes in brain activation during the acquisition of a multifrequency bimanual coordination task: from the cognitive stage to advanced levels of automaticity. The Journal of Neuroscience: the Official Journal of the Society for Neuroscience. 2005; 25: 4270–4278. https://doi.org/10.1523/JNEUROSCI.3866-04.2005
[45] Ruigrok AN, Salimi-Khorshidi G, Lai MC, Baron-Cohen S, Lombardo MV, Tait RJ, et al. A meta-analysis of sex differences in human brain structure. Neuroscience & Biobehavioral Reviews. 2014; 39: 34–50. https://doi.org/10.1016/j.neubiorev.2013.12.004
[46] Wu S, Fu Z, Wang S, Zheng F, Qiu W, Xu G, et al. Disrupted Functional Brain Network Architecture in Sufferers with Boxing-Related Repeated Mild Traumatic Brain Injury: A Resting-State EEG Study. Journal of Integrative Neuroscience. 2024; 23: 102. https://doi.org/10.31083/j.jin2305102
[47] Li L, Smith DM. Neural Efficiency in Athletes: A Systematic Review. Frontiers in Behavioral Neuroscience. 2021; 15: 698555. https://doi.org/10.3389/fnbeh.2021.698555
[48] Milton J, Solodkin A, Hlustík P, Small SL. The mind of expert motor performance is cool and focused. NeuroImage. 2007; 35: 804–813. https://doi.org/10.1016/j.neuroimage.2007.01.003
[49] Neubauer AC, Fink A. Intelligence and neural efficiency. Neuroscience and Biobehavioral Reviews. 2009; 33: 1004–1023. https://doi.org/10.1016/j.neubiorev.2009.04.001
[50] Bassett DS, Yang M, Wymbs NF, Grafton ST. Learning-induced autonomy of sensorimotor systems. Nature Neuroscience. 2015; 18: 744–751. https://doi.org/10.1038/nn.3993
[51] Napoli E, Masina F, Pezzetta R, Vanni F, Oliva G, Saccani MS, et al. Biomarkers of stroke recovery using EEG-based resting-state functional connectivity: a systematic review. Journal of Neuroengineering and Rehabilitation. 2026; 23: 142. https://doi.org/10.1186/s12984-026-01928-5
[52] Tachtsidis I, Scholkmann F. False positives and false negatives in functional near-infrared spectroscopy: issues, challenges, and the way forward. Neurophotonics. 2016; 3: 031405. https://doi.org/10.1117/1.NPh.3.3.031405
[53] Yücel MA, Lühmann AV, Scholkmann F, Gervain J, Dan I, Ayaz H, et al. Best practices for fNIRS publications. Neurophotonics. 2021; 8: 012101. https://doi.org/10.1117/1.NPh.8.1.012101
[54] Kirilina E, Jelzow A, Heine A, Niessing M, Wabnitz H, Brühl R, et al. The physiological origin of task-evoked systemic artefacts in functional near infrared spectroscopy. NeuroImage. 2012; 61: 70–81. https://doi.org/10.1016/j.neuroimage.2012.02.074
[55] Tagliazucchi E, Laufs H. Decoding wakefulness levels from typical fMRI resting-state data reveals reliable drifts between wakefulness and sleep. Neuron. 2014; 82: 695–708. https://doi.org/10.1016/j.neuron.2014.03.020
[56] Gagnon L, Perdue K, Greve DN, Goldenholz D, Kaskhedikar G, Boas DA. Improved recovery of the hemodynamic response in diffuse optical imaging using short optode separations and state-space modeling. NeuroImage. 2011; 56: 1362–1371. https://doi.org/10.1016/j.neuroimage.2011.03.001
[57] Brigadoi S, Ceccherini L, Cutini S, Scarpa F, Scatturin P, Selb J, et al. Motion artifacts in functional near-infrared spectroscopy: a comparison of motion correction techniques applied to real cognitive data. NeuroImage. 2014; 85: 181–191. https://doi.org/10.1016/j.neuroimage.2013.04.082
[58] Houwink A, Steenbergen B, Prange GB, Buurke JH, Geurts ACH. Upper-limb motor control in patients after stroke: attentional demands and the potential beneficial effects of arm support. Human Movement Science. 2013; 32: 377–387. https://doi.org/10.1016/j.humov.2012.01.007
[59] Pang MYC, Yang L, Ouyang H, Lam FMH, Huang M, Jehu DA. Dual-Task Exercise Reduces Cognitive-Motor Interference in Walking and Falls After Stroke. Stroke. 2018; 49: 2990–2998. https://doi.org/10.1161/STROKEAHA.118.022157
[60] Plummer P, Eskes G, Wallace S, Giuffrida C, Fraas M, Campbell G, et al. Cognitive-motor interference during functional mobility after stroke: state of the science and implications for future research. Archives of Physical Medicine and Rehabilitation. 2013; 94: 2565–2574.e6. https://doi.org/10.1016/j.apmr.2013.08.002
[61] Laver KE, Lange B, George S, Deutsch JE, Saposnik G, Chapman M, et al. Virtual reality for stroke rehabilitation. The Cochrane Database of Systematic Reviews. 2025; 6: CD008349. https://doi.org/10.1002/14651858.CD008349.pub5